VISIBILITY MONITORING USING CONVENTIONAL ROADSIDE CAMERAS: SHEDDING LIGHT ON AND SOLVING A MULTI-NATIONAL ROAD SAFETY PROBLEM

By

Raouf Babari
Université Paris-Est, LEPSIS, INRETS-LCPC
58 boulevard Lefebvre, 75015 Paris, France
Voice: +33 1 40 43 51 78
Fax: +33 1 40 43 54 99
raouf.babari@lcpc.fr

Nicolas Hautière
Université Paris-Est, LEPSIS, INRETS-LCPC
58 boulevard Lefebvre, 75015 Paris, France
Voice: +33 1 40 43 65 19
Fax: +33 1 40 43 54 99
nicolas.hautiere@lcpc.fr

Éric Dumont
Université Paris-Est, LEPSIS, INRETS-LCPC
58 boulevard Lefebvre, 75015 Paris, France
Voice: +33 1 40 43 53 76
Fax: +33 1 40 43 54 99
eric.dumont@lcpc.fr

Nicolas Paparoditis
IGN, Laboratoire MATIS
73 avenue de Paris, 94160 Saint-Mandé, France
Voice : +33 1 43 98 83 92
nicolas.paparoditis@ign.fr

James A. Misener[*]
California PATH, University of California, Berkeley
1357 S.46th Street, Bldg. 452
Richmond, CA 94804-4648
Voice: (510) 665-3612
Fax: (510) 665-3537
misener@path.berkeley.edu

Corresponding Author: Nicolas Hautière
Submission Date: 30th July 2010, revised 10th November 2010
Word Count (text body): 4284
Committee: AH010 Surface Transportation Weather

[*] Current affiliation: Booz Allen Hamilton, Richmond, CA 94804-4648, USA

ABSTRACT

The measurement of atmospheric visibility is an important element for road and air transportation safety. We propose in this paper a novel estimator of the atmospheric visibility by already-existing conventional highway cameras, with a technique based on the gradient magnitude obtained by applying Lambert's law with respect to changes in lighting conditions. The response of this estimator is calibrated by non-linear regression with data from a visibility-meter installed in a test site which has been instrumented with a camera. Through our technique, atmospheric visibility estimates are obtained with an average error of 30% for images taken in the day, with lighting conditions between 10 to 8,000 $cd.m^{-2}$ and visibility distances up to 15 km. Our emerging results indicate that a primary next step could be to deploy on current or future roadsides a practical implementation of our research results to determine local visibility for the benefit of drivers and the safety of our roads, while addressing the needs of meteorological observation and of air quality monitoring.

INTRODUCTION

In the presence of fog, haze or pollution, atmospheric visibility is reduced. This constitutes a common and vexing transportation problem for different public authorities in multiple countries throughout the world.

First, low visibility is obviously a problem of traffic safety. Road crashes which occur in fog are generally twice as severe as the average crash. According to the NOAA [1], in the United States there are approximately 700 annual fog-related fatalities, defined as occurring when visibility is less than ¼ mile (400 meters). Fog constitutes an equally important issue in France, a smaller country, with over 100 annual fatalities attributed to low visibility. Indeed, fog causes similar and significant problems on Northern America and French highways. It should be stressed that the solution lies not necessarily in better fog detection but in driver response to fog that is detected.

Indeed, the behavior of drivers in fog is often inappropriate (e.g., reduced headways, altered reaction times) but to understand the origins of these dangerous behaviors is difficult [2]. Different countermeasures have been tested to mitigate the impact of critically reduced visibility [3]. The California San Joaquin and Sacramento Valley regions are particularly adequate test-beds for such measures, because of the well-known Tule fog phenomenon. In the Stockton area of Caltrans District 10, the Caltrans Automated Warning System (CAWS) employs road-side weather stations and visibilitymeters to provide automated detection [4]. In District 6, Caltrans has installed the "Fog Pilot" system, which provides a high-technology solution every ¼ mile along a 12-mile (200-km) portion of State Route 99.

In addition to the safety problem, reduced visibility is cause of delays and disruption in air, sea and ground transportation for passengers and freight. On freeways, massive pile-ups create exceptional traffic congestions which sometimes force the operator to momentarily close the road. Fog-related road closures are not an uncommon subject for news headlines. Another example is the Heathrow airport which was blocked for three days during 2006 Christmas period. Such events have of course important economic impacts [5]. According to [6], in 1974 fog was estimated to have cost over roughly £120 millions at 2010 prices on the roads of Great Britain. This figure includes the cost of medical treatment, damage to vehicles and property, as well as the administrative costs of police, services and insurance, but they do not include the cost of delays to vehicles not directly involved in the accident.

Moreover, reduced visibility also creates environmental problems. Visibility is generally valued for environmental and aesthetic reasons that are difficult to express or quantify. Except for American national parks [7] and regulations on freeway advertisements, there are few places where visibility is considered a protected resource. Impaired visibility is also a symptom of environmental problems because it is evidence of air pollution [8]. In addition, it has been shown that impaired visibility and mortality are related [9]. According to the authors, visibility provides a useful proxy for the assessment of environmental health risks from ambient air pollutants and a valid approach for the assessment of the public health impacts of air pollution where pollutant monitoring data are scarce.

An ability to accurately monitor visibility helps resolve these problems. Important transportation facilities where safety is critical, such as airports, are generally instrumented for monitoring visibility with devices that are expensive and hence, scarce. Cost is precisely the reason why highway meteorological stations are seldom equipped with visibility metering devices. In this context, using already existing and ubiquitous highway cameras is of great interest, as these are low cost sensors already deployed for other purposes such as traffic monitoring [10]. Furthermore, introducing new functionalities into roadside cameras will make them multipurpose and thus more cost-effective, easing the deployment of these cameras along the roads.

In the United States, this potential has been identified by US DOT and was evaluated in the CLARUS Initiative [11,12], and these efforts may continue with the US DOT IntelliDrive program. In France, a similar initiative has been launched between LCPC (French Public Works Research Laboratory), Météo France and IGN (French National Geographical Institute), different French public research institutes dealing respectively with road operation, weather monitoring and forecasting, and geography and cartography. The French initiative aims at assessing the potential of highway cameras to monitor visibility for different applications ranging from safety hazard detection to air quality monitoring. This topic is also a matter of discussion and of potential collaboration between LCPC and California Partners for Advanced Transit and Highways (PATH) at Berkeley University.

In the future, such initiatives might make it possible to predict visibility reductions at the scale of a road itinerary, as it will soon be the case for airports [13].

BACKGROUND

Visibility measurement

Reduced visibility in the atmosphere is directly related to light scattering by air molecules and airborne particles. This tenet of physics is the basis of the operating principle of visibility-meters. There are two types of instruments for measuring atmospheric visibility: transmissometers and scatterometers. The transmissometer extrapolates the attenuation of a light beam emitted from a source to a receiver at a known path length in order to estimate the distance for which the emitted light is attenuated by 95 %. The transmissometer is also used to calibrate the scatterometer. A scatterometer assesses the dispersion of a light beam. Visibilitymeters can measure the meteorological visibility distance up to a few tens of kilometers with an accuracy of 10%. Some studies seek to exploit the photosensitive cells of fixed cameras to measure the meteorological visibility.

Related research

There are several general approaches to measuring meteorological visibility with a camera. The first is to detect the contrast of the most distant targets in a scene. For road safety, and visibility distances below 400 m, Hautière [14] assumes that the road is flat. He calculates all contrasts above 5% for objects obtained from the camera images. Using the geometric projection, he then estimates the distance to the farthest visible object with an accuracy of 10%. In another study Bäumer [15], in a panoramic scene, extracts gradients of targets whose distances are known based on a 2-dimensional map. In this work, ranges are longer because in meteorology, visibility distances are of the order of 10 km.

The second general approach to measuring meteorological visibility is based on machine learning, and requires a calibration phase with meteorological data collected with a visibilitymeter for several days and in different visibility conditions. In his study, Hallowell [12] exploits the road surveillance video camera network by proposing a fuzzy logic-based method which identifies four classes of visibility using image information. Other approaches which exploit machine learning seek to find the frequency response characteristics linking the image with visibility data. Indeed, Xie [16] and Liaw [17] seek the linear correlation between some indicator of contrast and meteorological visibility data. Xie [16] applies a low pass filter to the Fourier transform of the image. Hagiwara [18] also proposes a frequency operator WIPS which was proven to be well correlated with human perception. Liaw [17] acquires images at midday, seeking ways to reduce the influence of changing illumination.

The approach in this paper belongs to the second category. Indeed, an image-based estimator using a fixed Closed Circuit Television (CCTV) camera is proposed. Estimation results can be verified with meteorological visibility ground truth data collected with meteorological instruments. Unlike previous approaches, this one is stable to illumination change and therefore more indicative of the visibility. This article is organized as follows: Section 2 establishes the link between visibility and the gradient in the image; Section 3 clarifies the robustness of the approach; the results are presented in Section 4; a discussion follows, from which conclusions are drawn.

METHOD

Reduction in visibility by scattering

Although, the word "visibility" seems to be trivial, a more precise definition dedicated to meteorology is established through the theory of Koschmieder [19] which provides an analytic expression of the luminance *L* of an object observed from a distance *d* through an atmosphere with an extinction coefficient *k*. This is given by Equation 1.

$$L = L_0\, e^{-kd} + L_b\left(1 - e^{-kd}\right) \qquad (1)$$

The physical luminance of an object *L* reaching the camera is a linear combination of the intrinsic luminance of the object L_0 and the luminance of the sky behind the object L_b. The linear coefficient is an exponential function of the optical depth *kd* of the atmosphere which lies between the object and the camera (following Beer-Lambert law). From Equation 1, Duntley [19] derived a contrast attenuation law:

$$C = \left(L - L_b\right)/L_b = C_0 e^{-kd} \qquad (2)$$

The quantity *C* denotes the apparent contrast at a distance *d* of an object of luminance *L* against the sky in the background with a luminance L_b. C_0 is the intrinsic contrast of this object.

The International Commission on Illumination (CIE) recommends a threshold contrast of 5% to define visibility, so the meteorological visibility V_{Met}, expressed in Equation 3, is defined as the distance for which a black object ($C_0 = -1$) has a 5% contrast against the sky [20]:

$$V_{Met} = \frac{1}{k}\log(0.05) \approx 3/k \qquad (3)$$

Stability of contrast in Lambertian zones

In order to work with pixel intensity (or gray level) values given by a camera, the arguable assumption can be made that the response of the sensor is linear with a slope α. The intensity *I* of an object in the image can be expressed according to the value *L* of its physical luminance as shown in Equation 4:

$$I = \alpha\, L \qquad (4)$$

Using Equation 4 with Koschmieder'law in Equation 1 yields the following relation between the intensity *I* of a pixel, the optical depth *kd* of the atmosphere between the camera and the object in the direction subtended by this pixel, and the intensity A_∞ of the background sky:

$$I = I_0 \, e^{-kd} + A_\infty \left(1 - e^{-kd}\right) \tag{5}$$

Let us introduce the texture contrast C_{Texture}, defined for two adjacent points of intensity I_1 and I_2 found at the same distance $d_1=d_2=d$. Then from Equation 5, Equation 6 is obtained:

$$C_{\text{Texture}} = (I_2 - I_1)/A_\infty = \left[(I_{02} - I_{01})/A_\infty\right] e^{-kd} \tag{6}$$

The luminance of an object results from the reflection of both direct sunlight and light scattered through the atmosphere onto its surface. For objects with rough (and therefore Lambertian) surfaces, the reflected part of illuminance E is scattered evenly in all directions, and the luminance L is directly related to the albedo ρ of the surface material. In that case ρ is the diffuse reflection factor of the object. This is expressed by Lambert's law, where E is the illuminance on the surface:

$$L = \rho \, E/\pi \tag{7}$$

Hence, the expression of texture contrast for Lambertian objects is independent of illumination, and only depends on the object albedos ρ_1 and ρ_2, the distance d and the extinction coefficient k as shown in Equation 8:

$$C_{\text{Texture,Lambert}} = (\rho_2 - \rho_1) e^{-kd} \tag{8}$$

The main advantage of using the texture contrast is that its value is robust to variations of illumination in the scene since it is expressed as a function of albedo, an intrinsic characteristic of materials. Therefore, according to Equation 8, this contrast is expected to be a very strong indicator of the meteorological visibility despite illumination changes. There is no need to assume that all objects in the scene are Lambertian, only to select those that are.

Contrast as a module of Sobel gradient

The contrast defined above is a one-dimensional concept. In our case, however, the image is two-dimensional. The module of Sobel gradient, which indicates the value of the largest change from bright to dark at each pixel, is calculated with Equation 9:

$$G = \sqrt{G_x^2 + G_y^2} \tag{9}$$

The horizontal and vertical gradients, respectively G_x and G_y, are calculated by the convolution of the masks given in Equation 10:

$$G_x = \begin{bmatrix} +1 & 0 & -1 \\ 2 & 0 & -2 \\ +1 & 0 & -1 \end{bmatrix} * I \quad \text{and} \quad G_y = \begin{bmatrix} +1 & 2 & +1 \\ 0 & 0 & 0 \\ -1 & -2 & -1 \end{bmatrix} * I \tag{10}$$

The outcome of this processing is illustrated in Figure 1. The original image is shown in Figure 1 (a) and the gradient image – with edges enhanced as a direct result of the Sobel operator – is presented in Figure 1 (b).

(a) (b)

FIG.1 –Module of Sobel gradient of the image: (a) image in good visibility conditions; (b) Module of Sobel gradient of the same image.

Segmentation of Lambertian surfaces

Calculating the gradient of the image has been explained above. Those gradients which are most robust against illumination changes are extracted by selecting Lambertian surfaces within the scene. The best indicators of visibility variations are determined via this method, as shown with Equation 8. In practice, segmenting Lambertian areas in an image can be achieved by seeking the best linear correlation between the intensity changes of each pixel over time and the variations of illumination characterized by the sky luminance L_{scene}. The probability $P^L{}_{i,j}$ that the surface at pixel (i,j) is Lambertian can be calculated using the temporal correlation of Bravais-Pearson:

$$P_{i,j}^{L} = \operatorname{corr}\left(L_{i,j}, L_{\text{scene}}\right) \tag{11}$$

This is illustrated in Figure 2 where red denotes high correlation and, as a consequence, high probability for the surfaces to be Lambertian. Other robust methods exist to segment Lambertian surfaces in the image [21] but were found to be more complex to be used in practice.

FIG. 2 – Confidence that the area is Lambertian. Red determines the correlation between pixel intensity and scene illumination over time.

This segmentation allows discarding the specular reflections, such as sunlight on smooth surfaces, as well as shadows created by the movement of the sun during the day.

ESTIMATION OF METEOROLOGICAL VISIBILITY

Visibility estimation based on robust gradient

Let the estimator E equals the sum of all existing gradients in the image, absent any consideration of reflection (for the time being). This allows using Equation 12 and also corresponds to precedent in the literature [16, 17]. Now, let us consider the estimator of visibility E^L based on the sum of the module of Sobel gradient taken within Lambertian areas defined by Equation 13.

$$E^L = \sum_i \sum_j C_{0_{i,j}} \; e^{-kd_{i,j}} \tag{12}$$

$$E^L = \sum_i \sum_j P^L_{i,j} \; C_{0_{i,j}} \; e^{-kd_{i,j}} \tag{13}$$

To adjust the response function of the visibility estimator given by Equation 13, an empirical model described by Equation 14 is given. This function is the response of the estimator E^L according to changes in visibility conditions V_{Met} obtained by a visibilitymeter. Therefore, the response of the estimator $\tilde{E}^L$ of Equation 14 is adjusted by refining its parameters A and B. This is done by minimizing the quadratic error between the response function and the cloud of points relating the visibility estimator E^L from the image and the measured meteorological optical range V_{Met}:

$$\tilde{E}^L = A + B \log(V_{\mathrm{Met}}) \tag{14}$$

Correlation as a reliability indicator of visibility estimation

When the quadratic error is minimal, the correlation factor between estimator and visibility is close to 1. So, estimating the visibility V_{Met} by inversing the function $\tilde{E}^L$ will be closer to the reference values given by the visibilitymeter. The correlation factor constitutes an indicator of reliability in estimating this response function $\tilde{E}^L$.

Error due to model fitting

Parameters A and B must be adjusted so as to minimize the quadratic error χ^2 between the measured visibility V_{Met} and the visibility estimated by the function $V(\tilde{E}^L, A, B)$ with Equation 15:

$$\chi^2 = \sum_i \sum_j \left[V_{Met} - V\left(\tilde{E}^L, A, B\right) \right]^2 \tag{15}$$

Weighted fitting for low visibilities

Most of the time, images of low visibility will be rare compared to images of good visibility. Because the proposed model is empirical, this drives the largest error of the estimation in the more sparse low visibility data set. Therefore the curve fitting is weighted by giving more confidence to cases of low visibility as shown in Equation 16. Since the error increases linearly with visibility, the inverse of the accuracy $\sigma_{V\mathrm{Met}}$ is used as a confidence factor. This typically corresponds to 10% of the value of visibility V_{Met}. The results are shown in Figure 5.

$$\chi^2 = \sum_i \sum_j \frac{1}{\sigma_{V_{\mathrm{Met}}}} \left[V_{\mathrm{Met}} - V\left(\tilde{E}^L, A, B\right) \right]^2 \tag{16}$$

RESULTS

Image and data collection

Visibility and lighting data have been collected over several months. These data were matched with images taken from a camera. Indeed, a meteorological observatory was instrumented with a CCTV camera and a digital video recorder. The camera has the same quality as a typical roadside camera: 640 x 480 and a dynamic range of 8 bits per pixel. Images were acquired every 10 minutes for several months, with sky luminance between 0 and 10,000 cd.m^{-2} and meteorological optical range between 80 m to 50 km. Sample images with different weather conditions are shown in Figure 3. The luminance data were collected by means of a luminancemeter, and the visibility data were given by means of a scatterometer. Both instruments are common meteorological measurement systems often found on airports. Their operating principle was recalled in the background section. Sample data are shown in Figure 4.

(a) (b) (c)

FIG. 3 – Examples of images taken over several months under lighting conditions from 0 to 10,000 cd.m^{-2} and visibility conditions from 0 to 50 km: (a) Sunny day with shadows, (b) cloudy day, (c) low visibility.

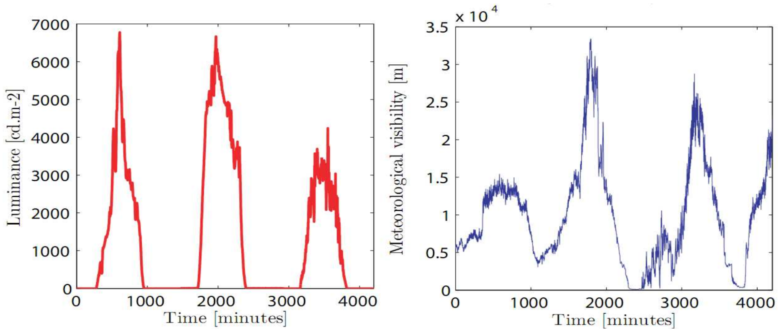

FIG. 4 – Sky luminance variation (red curve) and meteorological optical range variation (blue curve) during three days.

Comparison of results

The sum of the module of Sobel gradient computed from the images is plotted as a function of the measured meteorological visibility in Figure 5 (a). An instability and dispersion of the response of the estimator E can be observed. This instability is related to the change in lighting conditions, and this directly affects the values of object luminance in the scene and therefore it affects the resulting gradients. The instability is also related to the different reflections of sunlight on glass or other smooth, non-Lambertian surfaces. Because the imaged scene contains these elements, the module of Sobel gradient of the entire image cannot be a robust indicator of the measured meteorological visibility.

Results for the estimator $\tilde{E}^L$ are shown in Figure 5 (b). Points representing the visibility estimator $\tilde{E}^L$ as a function of the measured visibility V_{Met} follow an empirical law which appears to be logarithmic. For visibility distances below 1.5 km, the curve fit is weighted so as to reduce the influence of data with very high visibility. Results of this weighted curve fitting are shown in Figure 5 (c).

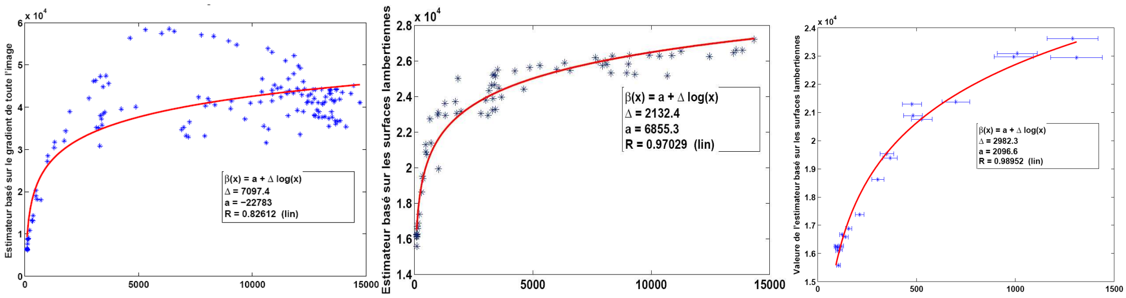

(a) (b) (c)

FIG. 5 – Logarithmic model fitting of the plot of the estimators as a function of reference visibilities: (a) E, sum of the module of Sobel gradient in the entire image; (b) $\tilde{E}^L$, sum of the module of Sobel gradients on Lambertian areas; (c) $\tilde{E}^L$, sum of the module of Sobel gradient considering Lambertian areas and with weighted fit for low visibility distances.

DISCUSSION

Meteorological visibility was estimated using an empirical response function. The values obtained are given in Table 1 for different applications, along with the average relative error $\Delta V/V$ from the reference values measured by a visibilitymeter. Processing the whole image results in a correlation factor of 0.82. For large visibility distances, this corresponds to an average relative error of 100 to 200%, meaning that the visibility estimation is irrelevant. Using gradients in Lambertian surfaces and a weighted fit for low visibility distance as described in this paper brings the average relative error down to 25%, which makes the estimation of the visibility more robust and reproducible over time. For visibility distances beyond 5 km, the average relative error becomes 33%, and it is as low as 10% for visibility distances below 400 m.

Despite these good results, the proposed model has still two main limitations. First, fixed camera is a requirement for the here proposed method which is intended to operate with roadside cameras such as those used for traffic surveillance. Second, the method does not deal currently with dynamic variance in the field of view such as traffic presence. This second limitation can be easily circumvented by using background modelling methods, as previously proposed by Hautière et al. in [14].

To implement this method of visibility estimation in a specific site, calibrating the logarithmic response curve is mandatory. In this aim, the simplest method consists in matching image contrasts with visisibility and luminance data collected by reference sensors (visibilitymeter and luminancemeter) during at least one foggy episode. For a massive deployment of the method on many different sites, more dedicated work is needed to simplify the calibration process so as to get rid of the reference sensors.

Application	**Highway fog**	**Fog**	**Haze**	**Air quality**	**Correlation**
Visibility range (Number of images)	0-400m 13 images	0-1000m 19 images	1000-5000m 26 images	5000-15000m 105 images	R^2 150 images
ΔV/V for E	22%	39 %	205 %	125 %	0.82
ΔV/V before weighted fit for $\tilde{E}^L$	11%	53 %	60 %	**33 %**	0.95
ΔV/V after weighted fit for $\tilde{E}^L$	**10%**	**25 %**	**26 %**	48 %	0.90

Table. 1 –Average relative error expressed in % as a function of range of application. Here the correlation factor is between 0.90 and 0.95 and corresponds to an error of 25% to 33%. For highway fog with less than 400 m visibility, the error is reduced to 10%.

CONCLUSION AND PERSPECTIVES

This study is aimed at a robust empirical law for estimating the meteorological visibility in daylight by means of a typical CCTV camera. The methodology presented in this paper is to link meteorological visibility to the sum of the module of Sobel gradient taken over Lambertian surfaces. It is demonstrated and validated that the proposed estimator is robust to changes in lighting conditions, and that any variation in measurement results are due to the variation of visibility in the atmosphere. Applying this estimator on real images acquired under a variety of visibility and lighting conditions, an estimated atmospheric visibility was obtained and then compared and validated with reference data collected with a meteorological instrument.

The approach for estimating visibility was also tested and validated under a large range of visibility and lighting conditions. It showed the relevance and the reproducibility of the approach. We believe therefore that this method for estimating meteorological visibility is easily deployable using the camera network already installed alongside highways throughout the world and therefore of high impact to traffic safety at marginal cost. Once deployed, this concept should increase the quality and the spatial accuracy of the visibility information and could feed weather forecasting systems. Importantly, our system may serve to inform drivers of relevant speed limits under low visibility conditions.

In future work, we will express errors in estimating visibility as a function of camera characteristics to ascertain the accuracy with which visibility can be estimated with current and future CCTV systems. We believe, however, that our work has given both a fundamental and practical basis to consider deployment of our potentially life-saving real-time roadside visibilitymeters.

ACKNOWLEDGMENTS

The work presented in this paper is co-funded by the LCPC and Météo-France. The authors wish to thank IGN for his contribution to the supervision of this work.

REFERENCES

[1] Whiffen , B., P. Delannoy , and S. Siok, 2004: Fog: Impact on road transportation and mitigation options. National Highway Visibility Conference, Madison, Wisconsin, 18-19 May 2004.

[2] Julie J. Kang, Rui Ni, and George J. Andersen. Effects of Reduced Visibility from Fog on

Car-Following Performance, Transportation Research Record: Journal of the Transportation Research Board, No. 2069, Transportation Research Board of the National Academies, Washington, D.C., 2008, pp. 9–15.

[3] Shepard, F.D.(1996) Reduced Visibility Due to Fog on the Highway, National Cooperative Highway Research Program, Synthesis of Highway Practice, 228.

[4] C. Arthur Mac Carley. Methods and Metrics for Evaluation of an Automated Real-Time Driver Warning System. *Transportation Research Record: Journal of the Transportation Research Board,* No. 1937, Transportation Research Board of the National Academies, Washington, D.C., 2005, pp. 87–95

[5] Tamara Pejovic, Victoria A. Williams, Robert B. Noland, Ralf Toumi. Factors affecting the frequency and severity of airport weather delays and the implications of climate change for future delays*, Transportation Research Record: Journal of the Transportation Research Board*, No. 2139, Transportation Research Board of the National Academies, Washington, D.C., 2009, pp. 97–106.

[6] Perry, A.H. and L.J. Symons. Highway Meteorology. University of Wales Swansea, Swansea, Wales, United Kingdom, 1991.

[7] Committee on Haze in National Parks and Wilderness Areas, Protecting visibility in national parks and wilderness areas. National Research Council, Washington, DC, 1993.

[8] Nicole Pauly Hyslop, Impaired visibility: the air pollution people see. *Atmospheric Environment*, Vol. 43, Issue 1, 2009, Pages 182-195.

[9] Thach,T.Q.,et al.,Daily visibility and mortality: Assessment of health benefits from improved visibility in Hong Kong. *Environmental Research*, 2010.

[10] Jacobs, N., W., B., Fridrich, N., Abrams, A., Miskell, K., Brswell, B., Richardson, A., Pless, R.: The global network of outdoor webcams: Properties and applications. ACM International Conference on Advances in Geographic Information Systems, 2009.

[11] Pisano, P.A.., Pol, J.S., Stern, A..D., Goodwin, L.C. CLARUS – The nationwide surface transportation weather observing and forecasting system. Presented at 84th Annual Meeting of the Transportation Research Board, Washington, D.C., 2005.

[12] Hallowell, R., Matthews, M., Pisano, P. An automated visibility detection algorithm utilizing camera imagery. In: 23rd Conference on Interactive Information and Processing Systems for Meteorology, Oceanography, and Hydrology (IIPS), 2007.

[13] Roquelaure, S., Tardif, R. Remy, S., Bergot, T. Skill of a Ceiling and Visibility Local Ensemble Prediction System (LEPS) according to Fog-Type Prediction at Paris-Charles de Gaulle Airport. *Weather and Forecasting*, 24, 2009, pp. 1511-1523.

[14] Hautière, N., Bigorgne, E., Bossu, J., Aubert, D., Meteorological conditions processing for vision-based traffic monitoring .In: International Workshop on Visual Surveillance, European Conference on Computer Vision, 2008.

[15] Bäumer, D., Versick, S., Vogel, B.: Determination of the visibility using a digital panorama camera. Atmospheric Environment, Vol. 42, 2008, pp. 2593-2602

[16] Ling Xie, Alex Chiu, and Shawn Newsam. Estimating atmospheric visibility using general purpose cameras. In International Symposium on Advances in Visual Computing, Part II, pages 356–367, Berlin, Heidelberg, 2008.

[17] J.J. Liaw, S.B. Lian, Y.F. Huang, and R.C. Chen. Atmospheric visibility monitoring using digital image analysis techniques. In International Conference on Computer Analysis of Images and Patterns, Pages 1204–1211, 2009.

[18] Hagiwara, T., Ota, Y., Kaneda, Y., Nagata, Y., Araki, K., Method of Processing Closed-Circuit Television Digital Images for Poor Visibility Identification. *Transportation Research Records: : Journal of the Transportation Research Board*, No. 1973, Transportation Research Board of the National Academies, Washington, D.C., 2007, pp. 95-104.

[19] Middleton, W.: Vision through the atmosphere. University of Toronto Press, 1952.

[20] CIE: International Lighting Vocabulary. Number 17.4., 1987.

[21] K. Seon Joo. Radiometric calibration with illumination change for outdoor scene analysis. In IEEE Conference on Computer Vision and Pattern Recognition, 2008.